Rapport BIPM-2000/04

Bureau International des Poids et Mesures

Comparison of the air-kerma standards of the ENEA-INMRI and the BIPM in the medium-energy x-ray range

D.T. Burns, M.P. Toni and M. Bovi

August 2000

Pavillon de Breteuil, F-92312 Sèvres Cedex

Comparison of the air-kerma standards of the ENEA-INMRI and the BIPM in the medium-energy x-ray range

by D.T. Burns, M.P. Toni* and M. Bovi*

Bureau International des Poids et Mesures, F-92312 Sèvres Cedex
* Istituto Nazionale di Metrologia delle Radiazioni Ionizzanti, ENEA C.R. Casaccia, CP 2400 – 00100 Rome, Italy

Abstract An indirect comparison has been made between the air-kerma standards of the ENEA-INMRI and the BIPM in the medium-energy x-ray range. The results show the standards to be in general agreement within the stated uncertainty, although there is evidence of a trend in the results at different radiation qualities.

1. Introduction

An indirect comparison has been made between the air-kerma standards of the Istituto Nazionale di Metrologia delle Radiazioni Ionizzanti (ENEA-INMRI) and the Bureau International des Poids et Mesures (BIPM) in the x-ray range from 100 kV to 250 kV. Two spherical cavity ionization chambers were used as transfer instruments. The measurements at the BIPM took place in September 1998 and those at the ENEA-INMRI in September and October 1998, using the reference conditions recommended by the CCRI [1].

2. Determination of the air-kerma rate

For a free-air ionization chamber standard with measuring volume V, the air-kerma rate is determined by the relation

$$\dot{K} = \frac{I}{\rho_{\text{air}} V} \frac{W_{\text{air}}}{e} \frac{1}{1 - g_{\text{air}}} \prod_i k_i \qquad (1)$$

where ρ_{air} is the density of air under reference conditions, I is the ionization current under the same conditions, W_{air} is the mean energy expended by an electron of charge e to produce an ion pair in air, g_{air} is the fraction of the initial electron energy lost by bremsstrahlung production in air, and $\Pi\, k_{\text{i}}$ is the product of the correction factors to be applied to the standard.

The values used for the physical constants ρ_{air} and W_{air} are given in Table 1. For use with this dry-air value for ρ_{air}, the ionization current I must be corrected for humidity and for the difference between the density of the air of the measuring volume at the time of measurement and the value given in the table[1].

3. Details of the standards

The air-kerma standard of the BIPM, described in [2], is of the conventional parallel-plate free-air chamber design in which the measuring volume V is defined by the diameter of the defining

[1] For an air temperature T, pressure P and relative humidity 50 % in the measuring volume, this involves a temperature correction T / T_0, a pressure correction P_0 / P, a humidity correction $k_{\text{h}} = 0.9980$, and the factor 1.0002 to account for the change in the compressibility of dry air between $T \sim 293$ K and $T_0 = 273.15$ K.

aperture and the length of the collecting region. The ENEA-INMRI standard has a telescopic cylindrical geometry, in which V is defined by the defining aperture and the difference between the extended and collapsed lengths. Details of the ENEA-INMRI standard, which has not previously been compared with the BIPM standard, are given in [3]. The main dimensions, the measuring volume and the polarizing voltage for each chamber are shown in Table 2.

Table 1. Physical constants used in the determination of the air-kerma rate

Constant	Value	u_i†
ρ_{air}‡	1.293 0 kg m^{-3}	0.000 1
W_{air} / e	33.97 J C^{-1}	0.001 5

† u_i is the relative standard uncertainty.

‡ Density of dry air at T_0 = 273.15 K and P_0 = 101 325 Pa.

Table 2. Main characteristics of the standards

Standard	BIPM	ENEA-INMRI
Aperture diameter / mm	9.939	10.008
Air path length / mm	281.5	403
Collecting length / mm	60.00	240.20†
Electrode separation / mm	180	6.5 - 22.5‡
Collector width / mm	200	9.5§
Measuring volume / mm^3	4 655.4	18 895†
Polarizing voltage / V	4 000	5 000

† The difference between the extended and collapsed lengths.

‡ This range arises because the axis of the cylindrical collector rod is displaced from the axis of the cylindrical outer electrode.

§ The diameter of the collector rod.

4. The transfer instruments

4.1 Determination of the calibration coefficient for a transfer instrument

The air-kerma calibration coefficient N_K for a transfer instrument is given by the relation

$$N_K = \frac{\dot{K}}{I_{tr}} \tag{2}$$

where $\dot{K}$ is the air-kerma rate determined by the standard using (1) and I_{tr} is the ionization current measured by the transfer instrument and the associated current-measuring system. The current I_{tr} is corrected to the standard conditions of air temperature, pressure and relative humidity chosen for the comparison (T = 293.15 K, P = 101 325 Pa and h = 50 %).

In general, to derive a comparison result from the calibration coefficients $N_{K,BIPM}$ and $N_{K,NMI}$ measured, respectively, at the BIPM and at a national measurement institute (NMI), differences

in the radiation qualities must be taken into account. Each quality used for the comparison has the same generating potential at each institute, but the half-value layers (HVLs) may differ. A radiation quality correction factor k_Q is derived for each comparison quality Q. This corrects the calibration coefficient $N_{K,\mathrm{NMI}}$ determined at the NMI into one which applies at the 'equivalent' BIPM quality and is derived by interpolation of the $N_{K,\mathrm{NMI}}$ values in terms of log(HVL). The comparison result at each quality is then taken as

$$\frac{\dot{K}_{\mathrm{NMI}}}{\dot{K}_{\mathrm{BIPM}}} = \frac{k_{\mathrm{Q}} N_{K,\mathrm{NMI}}}{N_{K,\mathrm{BIPM}}} \qquad (3)$$

In practice, the half-value layers normally differ by only a small amount and k_Q is close to unity.

4.2 Details of the transfer instruments

Two spherical cavity ionization chambers belonging to the ENEA-INMRI were used as transfer instruments for the comparison. Their main characteristics are given in Table 3. The reference point for each chamber was taken to be at the geometrical centre of the sphere. Each chamber was oriented so that the text marked on the chamber stem was facing away from the source.

Table 3. Main characteristics of the transfer chambers

Transfer chamber type	ENEA-T5	ENEA-T30
Serial number	05	105
Geometry	Spherical	spherical
External diameter / mm	9.8	44.0
Wall material	air-equivalent plastic	air-equivalent plastic
Wall thickness	0.07 g cm^{-2}	3 mm
Nominal volume / mm^3	380	28 000
Polarizing voltage / V	+200	+300
Typical polarity effect $I(+)$ / $I(-)$	1.002	1.000

5. Calibration at the BIPM

5.1 BIPM irradiation facility and reference radiation qualities

The BIPM medium-energy x-ray laboratory houses a constant-potential generator and a tungsten-anode x-ray tube with an inherent filtration of 2.3 mm aluminium. Both the generating potential and the anode current are stabilized using feedback systems constructed at the BIPM; this results in a very high stability and obviates the need for a transmission current monitor. The variation in the measured ionization current over the duration of a comparison introduces a relative standard uncertainty of typically 4×10^{-4}. The radiation qualities used in the range from 100 kV to 250 kV are those recommended by the CCRI [1] and are given in Table 4.

5.2 BIPM standard and correction factors

The reference plane for the BIPM standard was positioned at 1 200 mm from the radiation source, with a reproducibility of 0.03 mm. The standard was aligned on the beam axis to an

estimated uncertainty of 0.1 mm. The beam diameter in the reference plane is 105 mm for all radiation qualities, and an off-axis displacement of 0.1 mm changes the measured current by no more than 0.03 % at 100 kV.

Table 4. Characteristics of the BIPM reference radiation qualities

Generating potential / kV	100	135	180	250
Al filtration / mm	1.203 2	-	-	-
Cu filtration / mm	-	0.232 1	0.484 7	1.570 1
Al HVL / mm	4.027	-	-	-
Cu HVL / mm	0.148	0.494	0.990	2.500
μ_{air}† / 10^{-3} mm^{-1}	0.035 5	0.023 5	0.019 8	0.017 2
$\dot{K}_{BIPM}$ / mGy s^{-1}	0.21	0.20	0.29	0.38

† Air attenuation coefficient at 293.15 K and 100 000 Pa, measured at the BIPM for an air path length of 100 mm.

During the calibration of the transfer chambers, measurements using the BIPM standard were made at both polarities to correct for any polarity effect in the standard. The measured difference was typically 2×10^{-4} in relative value. The leakage current for the BIPM standard, relative to the ionization current, was measured to be less than 2×10^{-4}.

Table 5. Correction factors for the BIPM standard

Generating potential / kV	100	135	180	250	Relative standard uncertainty	
					u_{iA}	u_{iB}
Air attenuation k_a†	1.010 0	1.006 6	1.005 6	1.004 9	0.000 3	0.000 1
Scattered radiation k_{sc}	0.994 8	0.996 2	0.996 7	0.996 9	-	0.000 7
Electron loss k_e	1.000 0	1.002 3	1.005 2	1.007 8	-	0.001 0‡
Ion recombination k_s	1.000 5	1.000 5	1.000 5	1.000 5	0.000 2	0.000 1
Field distortion k_d	1.000 0	1.000 0	1.000 0	1.000 0	-	0.000 7
Aperture edge transmission k_l	0.999 9	0.999 8	0.999 7	0.999 6	-	0.000 1
Wall transmission k_p	1.000 0	1.000 0	0.999 9	0.998 8	0.000 1	-
Humidity k_h	0.998 0	0.998 0	0.998 0	0.998 0	-	0.000 3
$1 - g_{air}$	0.999 9	0.999 9	0.999 8	0.999 7	-	0.000 1

† These are nominal values for 293.15 K and 100 000 Pa; each measurement is corrected using the air temperature and pressure measured at the time.

‡ The value is less for the 100 kV and 135 kV radiation qualities.

The correction factors applied to the ionization current measured at each radiation quality using the BIPM standard, together with their associated uncertainties, are given in Table 5. The factor k_a corrects for the attenuation of the x-ray fluence along the air path between the reference plane and the centre of the collecting volume. It is evaluated using the measured air-attenuation coefficients μ_{air} given in Table 4. In practice, the values used for k_a take account of the temperature and pressure of the air in the standard at the time of the measurements. Ionization current measurements (both for the standard and for transfer chambers) are also corrected for changes in air attenuation arising from variations in the temperature and pressure of the ambient air between the radiation source and the reference plane.

5.3 Transfer chamber positioning and calibration at the BIPM

The reference point for each transfer chamber was positioned in the reference plane (1 200 mm from the radiation source), with a reproducibility of 0.03 mm. Each transfer chamber was aligned on the beam axis to an estimated uncertainty of 0.1 mm

The air temperature for the transfer chambers was measured using a calibrated thermistor positioned close to the chamber (outside the radiation field). The leakage current was measured before and after each series of ionization current measurements and a correction made using the mean value. For transfer chamber T30 the relative leakage current was less than 2×10^{-4}. For the smaller transfer chamber T5 the relative leakage current was up to 2.5×10^{-3}, but stable to better than 4×10^{-4} over the duration of a calibration.

The relative standard uncertainty of the mean of each of two series of ten measurements at each radiation quality was typically 4×10^{-4} and 7×10^{-5} for chambers T5 and T30, respectively. Taking into account the relative standard uncertainty of 4×10^{-4} arising from the typical repeatability over the duration of a comparison of current measurements using transfer chambers, a type A relative standard uncertainty of 5×10^{-4} is taken for all current measurements using the ENEA-INMRI transfer chambers at the BIPM.

Table 6. Characteristics of the ENEA-INMRI reference radiation qualities

Generating potential / kV	100	135	180	250
Al filtration / mm	3.48	4.08	4.06	4.02
Cu filtration / mm	-	0.18	0.51	1.72
Al HVL / mm	4.00	-	-	-
Cu HVL / mm	-	0.499	1.001	2.497
μ_{air}† / 10^{-3} mm^{-1}	0.035 5	0.023 8	0.020 3	0.017 8
$\dot{K}_{ENEA\text{-}INMRI}$ / mGy s^{-1}	1.1	1.2	1.1	1.2

† Air attenuation coefficient at 293.15 K and 100 000 Pa, measured at the ENEA-INMRI for an air path length of 150 mm.

6. Calibration at the ENEA-INMRI

6.1 ENEA-INMRI irradiation facility and reference radiation qualities

The medium-energy x-ray facility at the ENEA-INMRI comprises a constant-potential generator and a tungsten-anode x-ray tube with an inherent filtration of 3 mm beryllium. The output from a

potential divider is used to stabilize electronically the generating potential applied to the tube. In this way, variations in the x-ray output are maintained within 0.1 %. The residual variations are monitored by means of a transmission ionization chamber whose aluminized Mylar windows introduce a filtration of 3 mg cm^{-2}. The charge measuring system for the transmission monitor is similar to that for the standard and transfer chambers, and the stated uncertainty in ionization current measurements is that associated with current measurements relative to the transmission monitor. The characteristics of the ENEA-INMRI realization of the CCRI comparison qualities [1] are given in Table 6.

6.2 ENEA-INMRI standard and correction factors

The reference plane for the ENEA-INMRI standard was positioned at 1 000 mm from the radiation source, and the chamber was aligned on the beam axis to an estimated uncertainty of 0.1 mm. By means of a combined electro-optical distance meter, the positioning of the standard is reproducible to 0.01 mm, both in distance from the source and in alignment on the beam axis. The beam diameter in the reference plane is about 100 mm for all radiation qualities, and beam homogeneity is better than 0.2 % within a diameter of 50 mm

The ionization current for the standard is determined relative to that for the transmission monitor. The relative standard uncertainty of the mean of thirty such measurements was typically 2×10^{-4}.

Table 7. Correction factors for the ENEA-INMRI standard

Generating potential / kV	100	135	180	250	Relative standard uncertainty	
					$u_{i\mathrm{A}}$	$u_{i\mathrm{B}}$
Air attenuation k_a†	1.014 4	1.009 6	1.008 2	1.007 2	-	0.002 0
Scattered radiation k_{sc}‡	0.993	0.995	0.996	0.999	-	0.001 5
Electron loss k_e‡						
Ion recombination k_s§	1.003 4	1.003 6	1.003 3	1.003 1	0.000 1	0.000 5
Ion recombination k_s¶	1.002 7	1.002 8	1.002 3	1.002 9		
Field distortion k_d	-	-	-	-	-	-
Aperture edge transmission k_l	1.000 0	1.000 0	1.000 0	1.000 0	-	0.000 5
Wall transmission k_p	1.000 0	1.000 0	0.999 8	0.999 5	-	0.000 5
Humidity k_h	0.998 0	0.998 0	0.998 0	0.998 0	-	0.000 3
$1 - g_{air}$	0.999 9	0.999 9	0.999 8	0.999 7	-	0.000 1

† These are nominal values for 293.15 K and 100 000 Pa; each measurement is corrected using the air temperature and pressure measured at the time.
‡ Determined as the product k_{sc} k_e from data given in the literature [3].
§ For the collapsed free-air chamber (collector length 300.1 mm).
¶ For the extended free-air chamber (collector length 540.4 mm).

The polarity effect for the ENEA-INMRI standard is negligible with respect to the statistical uncertainty of ionization current measurements. During the calibration of the transfer chambers, measurements were made at both polarities to confirm the absence of a significant polarity effect. The relative leakage current was measured to be less than 2×10^{-4}.

The correction factors applied to the ionization current measured at each radiation quality using the ENEA-INMRI standard, together with their associated uncertainties, are given in Table 7. The correction factor k_a is evaluated using the measured air-attenuation coefficients μ_{air} given in Table 6. In practice, the values used for k_a take account of the temperature and pressure of the air in the standard at the time of the measurements. Ionization current measurements (standard and transfer chamber) are also corrected for variations in the temperature and pressure of the ambient air between the radiation source and the reference plane.

6.3 Transfer chamber positioning and calibration at the ENEA-INMRI

The reference point for each transfer chamber was positioned at the reference distance (at the ENEA-INMRI 1 000 mm from the radiation source), and each chamber was aligned on the beam axis. As noted above, positioning using the electro-optical distance meter is reproducible to 0.01 mm both in distance from the source and in alignment on the beam axis.

A calibrated quartz thermometer was used to measure the air temperature. The leakage current was measured before and after each series of ionization current measurements and a correction made based on the mean of these leakage measurements. The relative leakage current was less than 1×10^{-5} for the large transfer chamber T30 and up to 7×10^{-4} for the small transfer chamber T5.

The relative standard uncertainty of the mean of each of two series of ten measurements at each radiation quality was typically less than 5×10^{-4} for both chambers.

Table 8. Recombination correction factors for the transfer chambers

Generating potential / kV	100	135	180	250
Measurements at the BIPM				
I_{tr} for chamber T5 / pA	2.59	2.53	3.67	4.81
$k_{s,tr}$ for chamber T5	1.002 4	1.002 4	1.002 4	1.002 4
I_{tr} for chamber T30 / pA	199.6	197.3	284.7	369.4
$k_{s,tr}$ for chamber T30	1.003 5	1.003 5	1.003 8	1.004 2
Measurements at the ENEA-INMRI				
I_{tr} for chamber T5 / pA	13.8	14.6	14.2	15.7
$k_{s,tr}$ for chamber T5	1.002 5	1.002 5	1.002 5	1.002 5
I_{tr} for chamber T30 / pA	1 058.1	1 132.5	1 095.9	1 201.6
$k_{s,tr}$ for chamber T30	1.007 6	1.007 2	1.007 9	1.007 9

7. Additional corrections to transfer chamber measurements

7.1 Ion recombination

For both transfer chambers, the ion recombination correction is given by the relation

$$k_{\mathrm{s,tr}} = \frac{1}{1 - \mathrm{a} - \mathrm{b}I_{\mathrm{tr}}} \qquad (4)$$

where I_{tr} is the measured ionization current and a and b are constants determined empirically at the ENEA-INMRI for each transfer chamber. For chamber T5 the values are $\mathrm{a} = 2.41 \times 10^{-3}$ and $\mathrm{b} = 6.24 \times 10^{-6}$, and for chamber T30 $\mathrm{a} = 2.56 \times 10^{-3}$ and $\mathrm{b} = 4.46 \times 10^{-6}$. The measured values I_{tr} and the corresponding correction factors $k_{\mathrm{s,tr}}$ are given in Table 8.

7.2 Beam non-uniformity and polarity

No correction is applied at either laboratory for the radial non-uniformity of the radiation field. For the small transfer chamber T5 this will have a negligible effect. For the large chamber T30, this introduces a relative uncertainty which is estimated to be 1×10^{-3} at both the BIPM and the ENEA-INMRI.

Each transfer chamber was used with the same polarity at each laboratory and so no corrections are applied for polarity effects. The values for the polarity effect given in Table 3 are for information only.

7.3 Radiation quality correction factors k_Q

As noted in Section 4.1, slight differences in radiation qualities may require a correction factor k_{Q}. However, from Tables 4 and 6 it is evident that the radiation qualities at the BIPM and at the ENEA-INMRI are very closely matched in terms of HVL and so the correction factor k_{Q} is taken to be unity for all qualities, with a negligible uncertainty.

Table 9. Uncertainties associated with the standards

Laboratory	BIPM		ENEA-INMRI	
Relative standard uncertainty	$u_{i\mathrm{A}}$	$u_{i\mathrm{B}}$	$u_{i\mathrm{A}}$	$u_{i\mathrm{B}}$
Ionization current	0.000 3	0.000 2	0.000 8†	0.001 5
Volume	0.000 1	0.000 5	0.000 1	0.000 5
Positioning	0.000 1	0.000 1	-	0.000 1
Correction factors (excl. k_{h})	0.000 4	0.001 4	0.000 1	0.002 6
Humidity k_{h}	-	0.000 3	-	0.000 3
Physical constants	-	0.001 5	-	0.001 5
$\dot{K}_{\mathrm{lab}}$	0.000 5	0.002 1	0.000 8	0.003 4

† This is the uncertainty of the ionization current measurement relative to the transmission monitor.

8. Uncertainties

The uncertainties associated with the primary standards are listed in Table 9 and those for the comparison results in Table 10. The quoted uncertainties are representative of those associated with routine air-kerma calibrations at both institutions.

The relative combined standard uncertainty u_c of the ratio $\dot{K}_{\text{ENEA-INMRI}}/\dot{K}_{\text{BIPM}}$ takes into account correlations in the type B uncertainties associated with the physical constants and the humidity correction.

Table 10. Uncertainties associated with the comparison results

Laboratory	BIPM		ENEA-INMRI	
Relative standard uncertainty	$u_{i\text{A}}$	$u_{i\text{B}}$	$u_{i\text{A}}$	$u_{i\text{B}}$
$\dot{K}_{\text{lab}}$	0.000 5	0.002 1	0.000 8	0.003 4
Positioning of transfer chamber	0.000 1	0.000 1†	-	0.000 5†
I_{tr}	0.000 5	0.000 2	0.001 0‡	0.000 7
$N_{K,\text{lab}}$	0.000 7	0.002 1	0.001 3	0.003 5
$\dot{K}_{\text{ENEA-INMRI}}/\dot{K}_{\text{BIPM}}$	$u_c = 0.003\,8$§			

† For chamber T30, these increase to 0.001 0 at the BIPM and at the ENEA-INMRI to account for the radial non-uniformity of each beam.
‡ This is the uncertainty of the ionization current measurement relative to the transmission monitor.
§ Takes account of correlations in Type B uncertainties.

9. Results and discussion

The calibration coefficients determined at the BIPM and at the ENEA-INMRI are given in Table 11.

Table 11. Calibration coefficients for the transfer chambers

Generating potential / kV	100	135	180	250
Transfer chamber T5				
$N_{K,\text{ENEA-INMRI}}$ (pre-comp) / Gy μC^{-1}	81.13	80.92	79.71	78.77
$N_{K,\text{BIPM}}$ / Gy μC^{-1}	80.98	80.74	80.02	79.09
$N_{K,\text{ENEA-INMRI}}$ (post-comp) / Gy μC^{-1}	81.15	80.88	79.70	78.78
Transfer chamber T30				
$N_{K,\text{ENEA-INMRI}}$ (pre-comp) / Gy μC^{-1}	1.049 8	1.034 8	1.025 0	1.024 6
$N_{K,\text{BIPM}}$ / Gy μC^{-1}	1.050 3	1.034 0	1.031 2	1.028 7
$N_{K,\text{ENEA-INMRI}}$ (post-comp) / Gy μC^{-1}	1.049 6	1.033 5	1.025 6	1.025 6

For chamber T5, the pre- and post-comparison calibrations agree at the level of 3.0×10^{-4}, which is significantly better than one would expect from the given type A uncertainty of 1×10^{-3} (Table 10). For chamber T30, differences between the pre- and post-calibrations are larger and more consistent with the stated uncertainty. No systematic changes are observed between the pre- and post-calibration results.

The comparison results are summarized in Table 12. General agreement is observed, the mean ratio $\dot{K}_{\text{ENEA-INMRI}} / \dot{K}_{\text{BIPM}}$ for all eight comparisons (two chambers at four qualities) being 0.998 3 (relative standard uncertainty of the distribution 3.0×10^{-3}). The deviation from unity of this mean value is consistent with the stated comparison uncertainty of 3.8×10^{-3} (Table 10). However, both transfer chambers show a trend with radiation quality. The mean result at 100 kV and 135 kV is 1.000 9 (standard uncertainty 7×10^{-4}) and that at 180 kV and 250 kV is 0.995 7 (5×10^{-4}). This difference of 5×10^{-3} is statistically significant, but there is at present no explanation for this 'step'; all of the correction factors in Tables 5 and 7 are smoothly varying with radiation quality.

Table 12. Comparison results

Generating potential / kV	100	135	180	250
$\dot{K}_{\text{ENEA-INMRI}} / \dot{K}_{\text{BIPM}}$ using chamber T5	1.002 0	1.002 0	0.996 0	0.996 0
$\dot{K}_{\text{ENEA-INMRI}} / \dot{K}_{\text{BIPM}}$ using chamber T30	0.999 5	1.000 1	0.994 2	0.996 5
Mean $\dot{K}_{\text{ENEA-INMRI}} / \dot{K}_{\text{BIPM}}$	**1.000 7**	**1.001 1**	**0.995 1**	**0.996 3**

A summary of the results of BIPM comparisons of air-kerma standards for medium-energy x-rays, including the present comparison, is presented in Annex A. It can be noted from this data that the 'step' observed in the present comparison is not evident in other comparison results.

References

[1] BIPM, Qualités de rayonnement, CCEMRI(I), 1972, R15.

[2] BOUTILLON M., Mesure de l'exposition au BIPM dans le domaine des rayons X de 100 à 250 kV, 1978, *Rapport BIPM*-78/3.

[3] LAITANO R.F., TONI M.P., The primary exposure standard of ENEA for medium-energy x-rays: characteristics and measurement procedures, 1983, *ENEA Report* RT/PROT(83)27.

Annex A

The results of BIPM comparisons of air-kerma standards for medium-energy x-rays are presented in Table A.1. For NMIs which have compared their standard more than once with the BIPM, only the results of the most recent comparison are included. The same data are presented in graphical form in Figure A.1.

Table A.1 Results of BIPM medium-energy x-ray comparisons, expressed as $\dot{K}_{\mathrm{NMI}} / \dot{K}_{\mathrm{BIPM}}$.

NMI	Country	Date	Generating potential / kV			
			100 kV	135 kV	180 kV	250 kV
OMH	Hungary	1975	1.0040	1.0013	0.9994	0.9961
PTB	Germany	1975	1.0016	1.0003	1.0002	1.0016
CSIR	S Africa	1976	0.9969	1.0042	1.0008	1.0049
BEV	Austria	1982	0.9988	0.9980	0.9979	0.9960
ARL	Australia	1988	1.0037	1.0046	1.0029	1.0044
NIST	USA	1991	1.0020	1.0021	1.0010	0.9997
NMi	Netherlands	1991	1.0018	0.9975	0.9950	0.9937
GUM	Poland	1994	0.9985	0.9968	0.9959	0.9944
NPL†	UK	1997	0.9958	0.9928	0.9933	0.9888
BNM-LCIE	France	1998	0.9901	0.9979	0.9996	0.9980
ENEA	Italy	1998	1.0007	1.0011	0.9951	0.9963

† The results for this laboratory are provisional; BIPM report still in preparation.

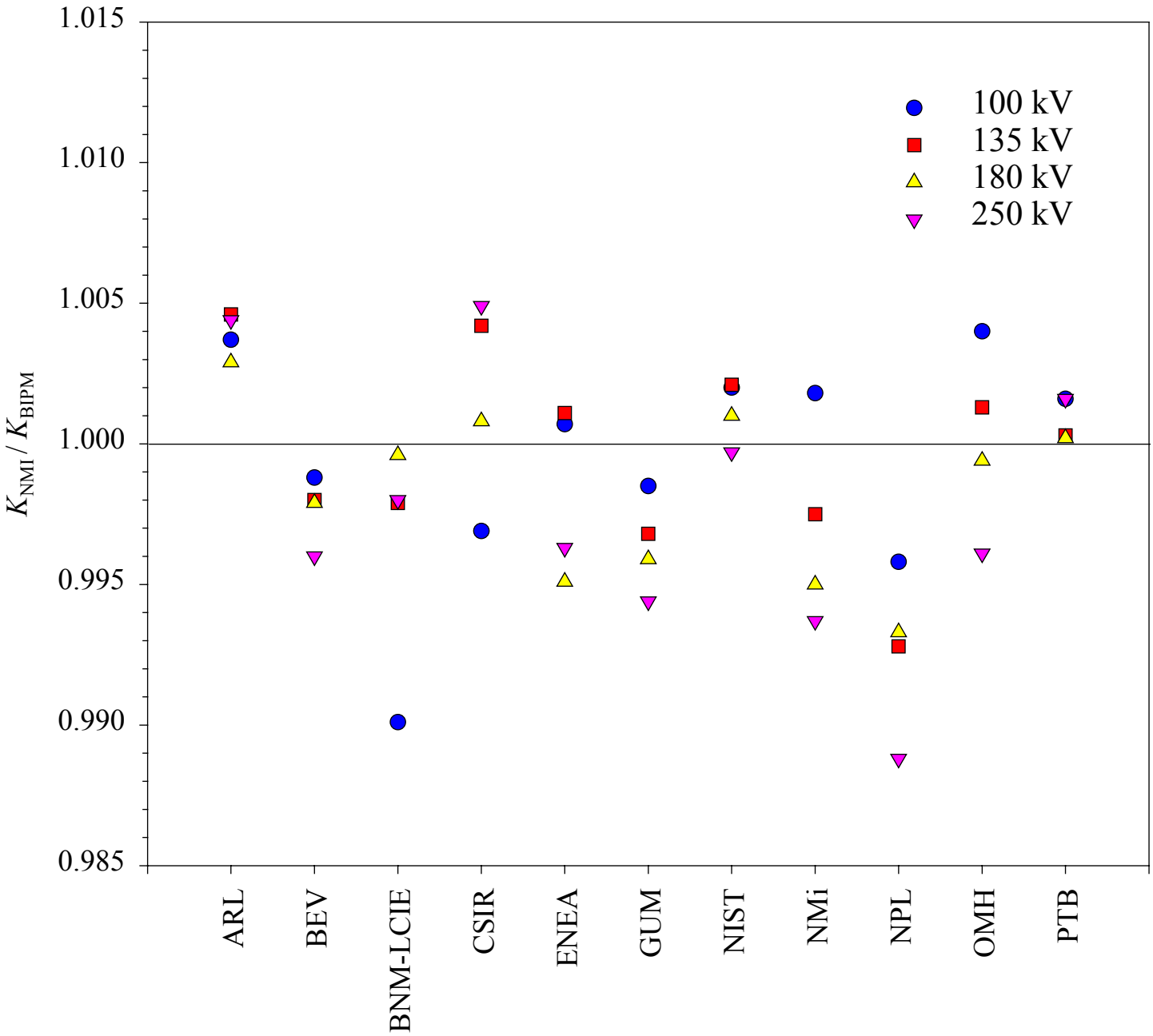

Figure A.1. Results of BIPM medium-energy x-ray comparisons, expressed as the ratio of the air-kerma rate determined by the NMI standard to that determined by the BIPM standard. The results for the NPL are provisional.